International Journal of Fatigue 42 (2012) 88–94

Contents lists available at ScienceDirect

International Journal of Fatigue

journal homepage: www.elsevier.com/locate/ijfatigue

Analysis of fatigue crack growth in an attachment lug based on the weight function technique and the UniGrow fatigue crack growth model

S. Mikheevskiy [a,*], G. Glinka [a], D. Algera [b]

[a] University of Waterloo, Department of Mechanical Engineering, Waterloo, ON, Canada N2L 3G1
[b] Technical Data Analysis, Inc., 7600A Leesburg Pike, Suite 204, Falls Church, VA 22043, United States

ARTICLE INFO

Article history:
Received 15 October 2010
Received in revised form 4 April 2011
Accepted 14 July 2011
Available online 23 July 2011

Keywords:
Fatigue crack growth
Corner crack
Load shedding
Weight function

ABSTRACT

A generalised step-by-step procedure for fatigue crack growth analysis of structural components subjected to variable amplitude loading spectra has been presented. The method has been illustrated by analysing fatigue growth of planar corner crack in an attachment lug made of Al7050-T7451 alloy.

Stress intensity factors required for the fatigue crack growth analysis were calculated using the weight function method. In addition, so-called "load-shedding" effect was accounted for in order to determine appropriate magnitudes of the applied stress intensity factors. The rate of the load shedding was determined with the help of the finite element (FE) method by finding the amount of the load transferred through the cracked ligament. The UniGrow fatigue crack growth model, based on the material stress–strain behaviour near the crack tip, has been used to simulate the fatigue crack growth under two variable amplitude loading spectra. The comparison between theoretical predictions and experimental data proved the ability of the UniGrow model to correctly predict fatigue crack growth behaviour of two-dimensional planar cracks under complex stress field and subjected to arbitrary variable amplitude loading.

1. Introduction

Lug-type joints are often used to connect components in various mechanical systems. Since the lug is usually attached to the fork by a single bolt or pin without clamping, it is easy to mount and does not produce any additional local bending moments. However, cracks or other discontinuities can be initiated due to corrosion, material imperfection, manufacture defects, or fatigue. Despite the improved damage tolerance design procedures and usage of non-destructive inspection techniques, unsafe cracks may still be present in lugs and go unchecked during regular maintenance inspections. If such a crack or flow occurs in the region of high stress concentration near the lug hole it can quickly propagate and significantly reduce the operational life of a component. In order to ensure operational safety of a structure it is necessary to perform fatigue crack growth analysis assuming the possibility of fatigue crack initiation and growth. A number of analytical and experimental studies have been performed over last three decades, aiming at investigating the fatigue behaviour of attachment lugs under both constant and variable amplitude loading [1–3].

The approach discussed below is based on the weight function method [4] and the UniGrow fatigue crack growth model proposed by Noroozi et al. [5] and extended by Mikheevskiy and Glinka [6]. The list of main steps required for the fatigue analysis of an attachment lug is given below:

- Collect material information (modulus of elasticity, cyclic stress–strain curve, constant amplitude fatigue crack growth data).
- Determine required stress field in an un-cracked lug induced by the applied load (with the help of the FE-finite element analysis or any other method).
- Calculate the load shedding parameter for several different crack sizes.
- Determine the crack shape and calculate stress intensity factors using the weight function method and the load shedding correction factor for each cycle of the loading spectrum.
- Determine the instantaneous fatigue crack growth rate using the UniGrow fatigue model.

2. Geometry of the component and material data

The attachment lug [7] was made of Al 7050-T7451 aluminium alloy material. The constant amplitude fatigue crack growth data for this material was collected from several literature sources [7–9]. Eight constant amplitude (CA) fatigue crack growth (FCG) data sets, obtained at six different stress ratios, were selected as

* Corresponding author.
E-mail address: volchishka@gmail.com (S. Mikheevskiy).

0142-1123/$ - see front matter © 2011 Elsevier Ltd. All rights reserved.
doi:10.1016/j.ijfatigue.2011.07.006

the reference for subsequent fatigue crack growth and fatigue life analysis (Fig. 1).

The geometrical configuration and dimensions of the lug tested [7] under variable amplitude loading spectra are shown in Fig. 2. The lug was 10 mm thick (t = 10 mm) with the hole radius of 13 mm (R_i = 13) and the outer radius of 35 mm (R_o = 35). A beryllium copper bushing was installed with 0.1 mm diametrical interference between the lug and the pin.

A quarter-circular corner crack (Fig. 2) with initial dimensions of $a = c$ = 1 mm was artificially made in the lug whose growth monitored later. As soon as the corner crack propagated through the entire thickness of the specimen it quickly transformed into the classical edge crack emanating from a hole. Therefore special stress intensity factor solution was needed in order to appropriately model the fatigue crack shape evolution. A more detailed description of the specimen and the testing procedure can be found in the original work of Kim et al. [7].

3. The stress field in the critical cross section of the attachment lug

The stress field in the un-cracked attachment lug was determined with help of the finite element method. The stress field was used to determine the stress intensity factor by using the weight function method. The stress field in the potential crack plane of an un-cracked lug is shown in Fig. 3. The variation of through thickness stress was assumed to be small due to relatively large diameter of the lug-hole compared to the lug thickness.

The same lug was also analysed by Kim et al. [7] using the boundary element method. As one can see the results are almost identical and the elastic gross stress concentration factor was around five.

4. Determination of the stress intensity factor

The geometrical shape of the growing fatigue crack, as was mentioned earlier, was changing from quarter-circular to an edge one. Therefore, the stress intensity factor analysis consisted of several stages appropriate for various crack shapes as shown in Fig. 4.

4.1. The stress intensity factor (SIF) for quarter-elliptical crack

The quarter-elliptical corner crack was analysed first using two-dimensional generalised weight function proposed by Glinka and Shen [10]. Strictly speaking, the fatigue growth of a corner or any other planar crack depends on the value of stress intensity factor at each point along the crack front. In the analysis below it is assumed that the crack shape remained quarter-elliptical, and therefore only two surface points 'A' and 'B' (Fig. 4) needed to be considered. It has been shown [10] that stress intensity factors at point 'A' and point 'B' can be determined using the integrals involving the stress field and appropriate weight functions.

$$K^{A} = \int_0^c \sigma(x) m_A(x, c, c/a) dx$$
$$K^{B} = \int_0^c \sigma(x) m_B(x, c, c/a) dx \quad (1)$$

where '$\sigma(y)$' is the stress distribution through the width of the specimen, 'c' and 'a' are the crack dimensions as shown in Fig. 2. The weight function expressions 'm_A' and 'm_B' are given in reference [10].

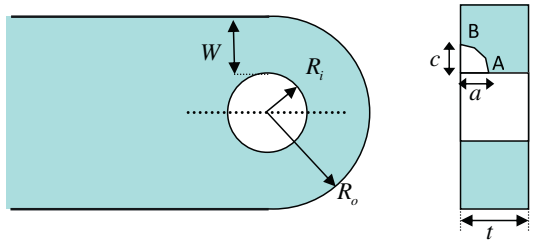

Fig. 2. Geometry of the attachment lug with an initial quarter-circular corner crack (W = 22 mm, R_i = 13 mm, R_o = 35 mm and t = 20 mm).

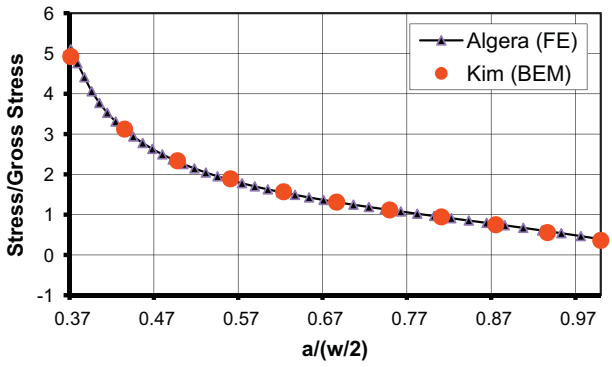

Fig. 3. Stress distribution in un-cracked lug.

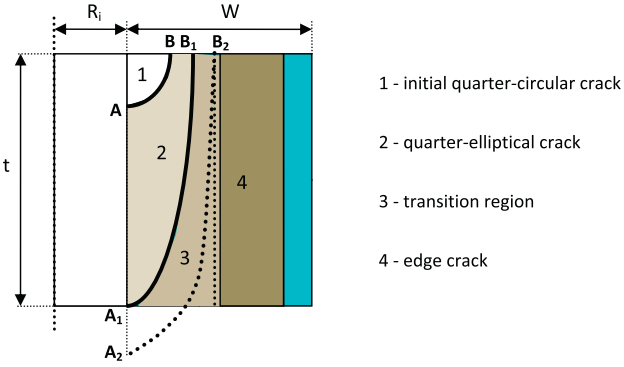

Fig. 4. Evolution of the fatigue crack in attachment lug.

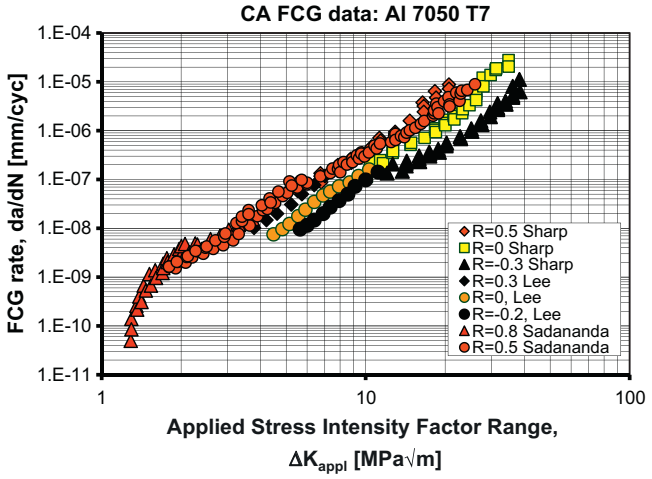

Fig. 1. Experimental constant amplitude fatigue crack growth data for the Al 7050 T7 alloy in terms of the applied stress intensity range.

While the fatigue crack propagates point 'B' moves into the region of lower stresses as shown in Fig. 3. On the other side, stresses for point 'A' stay the same since they are uniformly distributed through the thickness. Therefore, it is reasonable to expect higher stress intensity factors and fatigue crack growth rates at point 'A' resulting in the change of the initial crack shape from quarter-circular to quarter-elliptical and elongated along the thickness. The variation of stress intensity factors at points 'A' and 'B' obtained as a function of the crack length 'a' for the aspect ratio $a/c = 1$ and the applied stress $S = 30$ MPa is shown in Fig. 5.

4.2. The stress intensity factor for the transition crack

When the corner crack breaks through the whole thickness of the lug it turns into an edge crack. Unfortunately, the weight function enabling smooth transition from corner to edge crack as shown Fig. 4 (Region 3) has not been derived yet. Thus, the following approach has been adopted.

The two-dimensional weight functions (Eq. (1)) have been derived for stress fields which are uniform through the thickness. Therefore, despite the fact that they depend on both crack dimensions 'a' and 'c', they do not depend on the through thickness stress variation. Thus, the crack was analysed first as a corner crack until the length 'a' exceeded (see Figs. 2 and 4) the lug thickness 't' by 20%, i.e. when $a > 1.2t$. After that stage the crack was modelled as an edge crack with its initial depth 'c' coinciding with the location of point B2 (Fig. 4).

4.3. Thestress intensity factor for an edge crack emanating from a hole

An edge crack in a lug is less difficult to analyze than a corner one, and therefore, several attempts have been made in the past aiming to investigate the stress intensity factor for only an edge crack in a lug. Aberson and Anderson [11] used finite element analysis with a crack tip singularity elements, Impellizeri and Rich [12] employed the weight function method, and Schijve and Hoeymaker [13] found the empirical solution based on the fatigue crack growth data.

Glinka and Shen [14] have derived the general form of one-dimensional weight function (Eq. (3)) which was used to calculate the stress intensity factor (Eq. (4)) for the edge crack in the lug based on the actual stress field $\sigma(x)$ obtained from finite element analysis (Fig. 3) of un-cracked lug. The stress distribution $\sigma(x)$ in the prospective crack plane was obtained from the finite element analysis. The load force P in the hole was replaced by a pressure distribution resulting from the contact between the pin and the hole in the lug and it was simulated by imposing restrains on radial

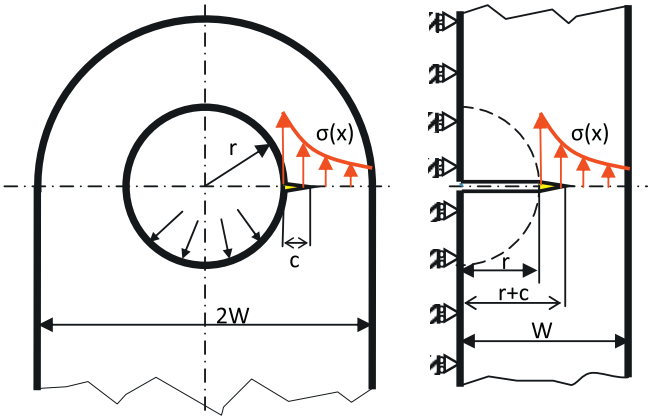

Fig. 6. Edge crack in attachment lug and the weight function model.

displacement in the region of the contact between the pin and the lug.

$$m(x,c) = \frac{2}{\sqrt{2\pi(c-x)}}\left[1 + M_1\left(1-\frac{x}{c}\right)^{\frac{1}{2}}\right. \tag{2}$$

$$\left. + M_2\left(1-\frac{x}{c}\right)^{1} + M_3\left(1-\frac{x}{c}\right)^{\frac{3}{2}}\right] \tag{3}$$

$$K = \int_0^c \sigma(x)m(x,c)dx \tag{4}$$

Coefficients M_1, M_2, and M_3 were derived for an edge crack in a finite plate width with fixed one edge as shown in Fig. 6.

The stress intensity factor solution obtained from the weight function has been compared to the solution calculated by Kim et al. [7] by the using boundary element method and both sets of results are shown in Fig. 7. The weight function based stress intensity factors seem to be slightly conservative while compared with the boundary element method.

5. The load shedding

The weight function method described in Section 4 requires using the stress field from un-cracked body induced by the applied load in the prospective crack plane (Fig. 3). This approach is valid as long as the cracked section is taking all the time the same amount of the resultant load while the crack propagates through the cross section. However, in the case of a single crack in a lug (Fig. 8), the cracked section "$W2$" becomes less rigid than

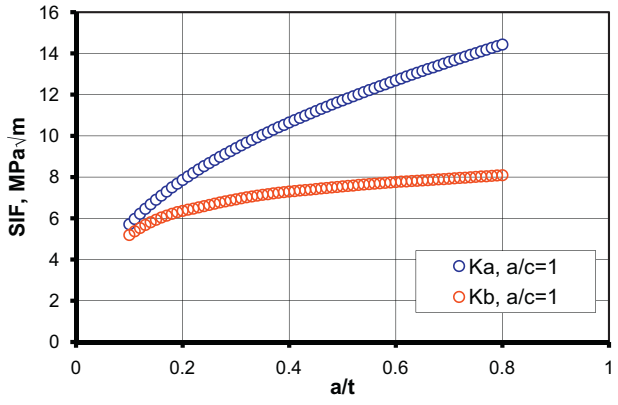

Fig. 5. SIF for quarter-circular crack obtained using generalised two-dimensional weight function.

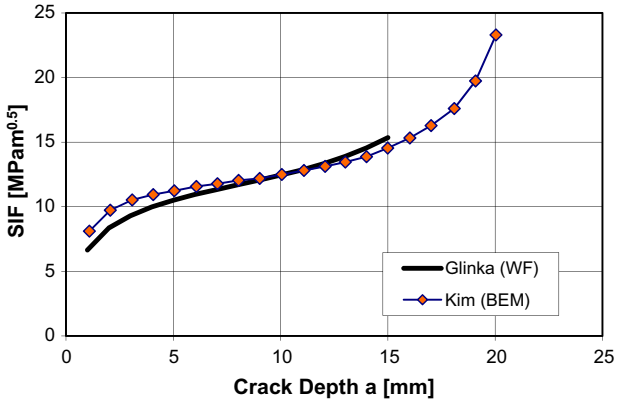

Fig. 7. Comparison of stress intensity factors obtained from the weight function and the boundary element method (nominal gross stress $S = 30$ MPa).

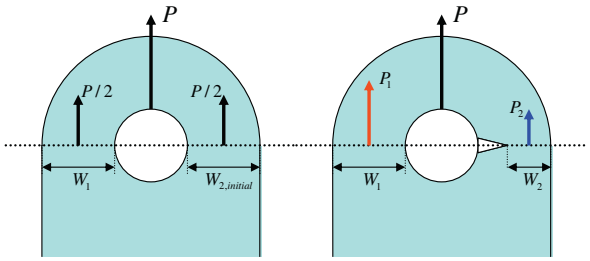

Fig. 8. Schematic illustration of the load shedding effect.

un-cracked section "*W*1", and part of the applied load is transferred to section "*W*1". This situation would not happen in the case of two symmetric cracks because both sections have to hold the same amount of load equal to the half of the load applied to the lug.

It has been shown using finite element analysis that this effect is relatively small as long as crack stays quarter-elliptical, but becomes significant when crack breaks through the entire thickness of the lug.

Introduction of the load shedding coefficient, LS(c/W), enables to estimate the amount of load taken by the cracked section '*W*2' and estimate the actual load (Fig. 8).

$$P_2 = \mathrm{LS}\left(\frac{c}{W}\right)\cdot\frac{P}{2} \quad \text{where } \mathrm{LS}(0) = 1 \tag{5}$$

Since the magnitude of the stress field in a ligament depends only on the magnitude of the load transferred through the ligament the instantaneous stress distribution can be written as

$$\sigma(x) = \mathrm{LS}\left(\frac{c}{W}\right) * \frac{P}{2} * \sigma_n(x) \tag{6}$$

where $\sigma_n(x)$ is the stress field/distribution normalised obtained for the unit load. Thus, the stress intensity factor for a single edge crack in a lug can be subsequently written in the form:

$$K(c) = \int_0^c \mathrm{LS}\left(\frac{c}{W}\right) * \frac{P}{2} * \sigma_n(x) * m(c,x)dx \tag{7}$$

Taken into account the fact that the load shedding coefficient controls only the magnitude of the stress field and does not depend on the '*x*' coordinate, the final equation for the resultant stress intensity factor can be written as:

$$K(c) = \mathrm{LS}\left(\frac{c}{W}\right)\cdot K_{WF}(c) \tag{8}$$

where $K_{WF}(c)$ is the standard solution obtained by using the weight function method as described in Section 4. The main challenge is to determine the load shedding parameter, LS(c/W), as a function of the crack size. Therefore, complete 3D finite element analysis was carried out for three different edge cracks of 5 mm, 10 mm, and 15 mm deep. Accurate modelling of the stress field near the crack tip was not necessary in those cases, and therefore, coarse finite element mesh could be used over the entire ligament. The stress distributions obtained from the FE analyses are presented in Fig. 9. The resultant force P_2 transferred by the cracked ligament was determined by integrating appropriate stress field acting in the remaining cross section.

$$P_2 = \iint_s \sigma(x,y)dx\ dy = t\int_W \sigma(x)dx \tag{9}$$

As one can see, stresses in the un-cracked section went up as the crack propagated through the other ligament. This means that the resultant force P_2 in the cracked ligament must have got decreased and the amount of the decrease could be measured by the load shedding factor LS.

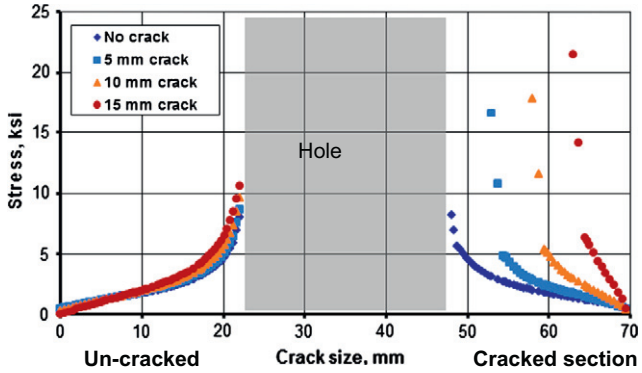

Fig. 9. Stress fields obtained for three different crack lengths.

The variation of the load in the cracked and un-cracked ligament of the lug as a function of the crack depth '*c*' is shown in Fig. 10. The results show that at the crack depth c = 15 mm the load transferred by the cracked cross-section was reduced by around 20%, which resulted in approximately 55% reduction in the fatigue crack growth rate.

The load shedding parameter was subsequently fitted into following expression

$$\mathrm{LS}\left(\frac{c}{W}\right) = 1 - A\left(\frac{c}{W}\right)^q \tag{10}$$

with parameters A = 0.4 and q = 1.3. It has been shown that Eq. (10) fits well into the data obtained from the FE analysis for relative crack depths $0 < c/i < 0.8$.

The final expression for the edge crack stress intensity factor was obtained by including all the information discussed above into Eq. (3).

$$K(c) = \left[1 - 0.4\left(\frac{a}{W}\right)^{1.3}\right]\int_0^c \sigma(x)\cdot m(c,x)dx \tag{11}$$

Based on Eq. (11) the maximum applied stress intensity factor, $K_{\max,\mathrm{appl}}$ and the applied stress intensity range, ΔK_{appl}, could be determined for each cycle of the applied loading spectrum. As mentioned in Section 2, the UniGrow fatigue model was used for the determination of the instantaneous fatigue crack growth rate and crack increments induced by each individual loading cycle.

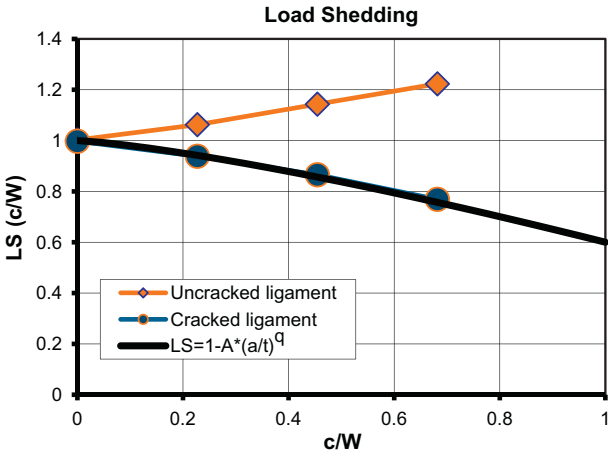

Fig. 10. Load shedding coefficient.

6. Basics of the UniGrow fatigue model

The UniGrow fatigue crack growth model, initially proposed by Noroozi et al. [5], is based on the idea that the fatigue process near cracks and notches is governed by highly concentrated strains and stresses in the notch/crack tip region. Therefore, the fatigue crack growth can be subsequently considered as a process of successive crack increments resulting from material damage in this region.

According to the micro-support concept of Neuber [15], the real material can be modelled as a set of elementary particles or material blocks of a finite dimension, $\rho*$. The idea of elementary material blocks was also postulated by Forsyth [16] based on microscopic observations of the fatigue crack front advance. The assumption of the elementary material block implies that the actual stress–strain and fatigue response of the material near the crack tip is such as the crack had a blunt tip with the radius of $\rho*$. It means that it might be reasonable to model the crack, within the continuum mechanics framework, as a sharp notch with the tip radius $\rho*$. Therefore, the classical notch stress–strain analysis techniques can be applied in order to determine stresses and strains in the crack tip region.

The following assumptions and computational rules form the base for the UniGrow fatigue crack growth model.

- The material consists of elementary blocks of a finite dimension $\rho*$.
- The fatigue crack is regarded as a notch with the tip radius $\rho*$.
- The analysis is based on the Ramberg-Osgood (cyclic) [17] and Manson-Coffin (fatigue) [18] material properties.
- The number of cycles to fail the material over the distance $\rho*$ can be obtained using the Smith–Watson–Topper damage parameter [19] and the Manson-Coffin fatigue curve.
- The instantaneous fatigue crack growth rate can be expressed as $da/dN = \rho*/N$.

Based on the assumptions stated above Noroozi et al. [5] have analytically derived the fatigue crack growth expression in the form of

$$\frac{da}{dN} = C\left((K_{\max,\mathrm{appl}} + K_r)^p(\Delta K_{\mathrm{appl}} + K_r)^{1-p}\right)^m \tag{12}$$

where $K_{\max,\mathrm{appl}}$ and ΔK_{appl}, are the applied maximum stress intensity factor and the stress intensity range respectively, and K_r is the residual stress intensity factor accounting for the effect of crack

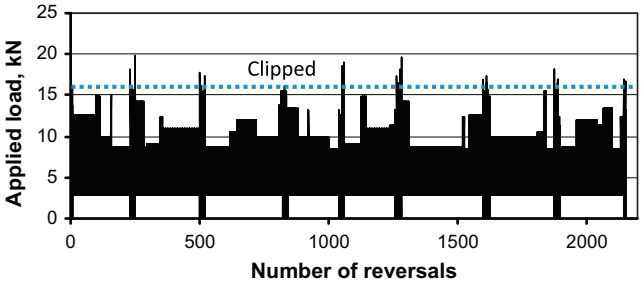

Fig. 12. Applied loading spectrum.

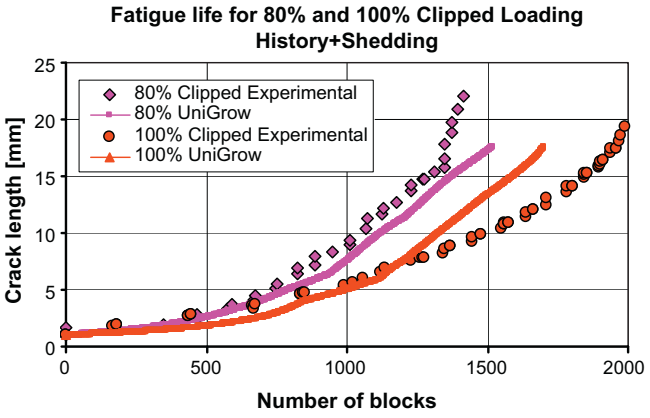

Fig. 13. Fatigue crack growth predictions and the experimental data for the original and the truncated load spectrum.

tip residual stresses resulting from reversed plastic deformations. For the simplicity, Eq. (12) can be rewritten as

$$\frac{da}{dN} = C(\Delta\kappa)^m;\ \Delta\kappa = (K_{\max,\mathrm{appl}} + K_r)^p(\Delta K_{\mathrm{appl}} + K_r)^{1-p} \tag{13}$$

where $\Delta\kappa$ is total two-parameters driving force.

A very similar fatigue crack growth equations has been proposed by Walker [20] and Dinda and Kujawski [21] based on empirical fitting of observed constant amplitude fatigue crack growth data. However, Walker and Kujawski expressions did not

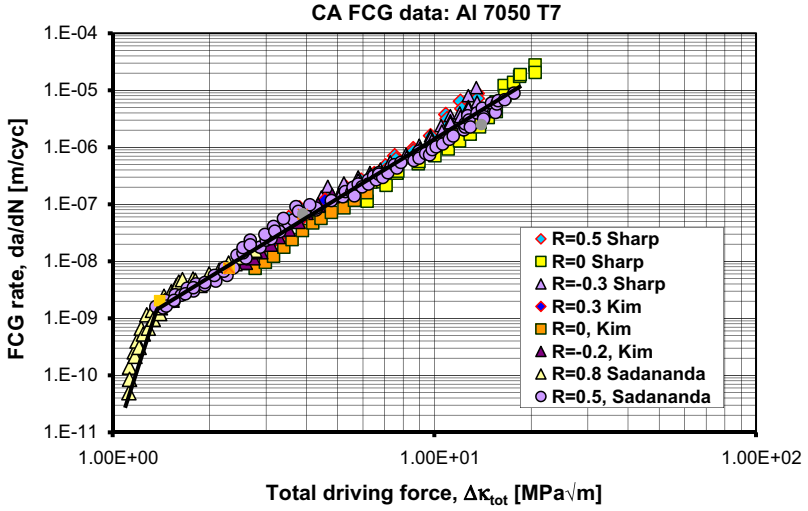

Fig. 11. Fatigue crack growth rate in terms of total two-parameter driving force.

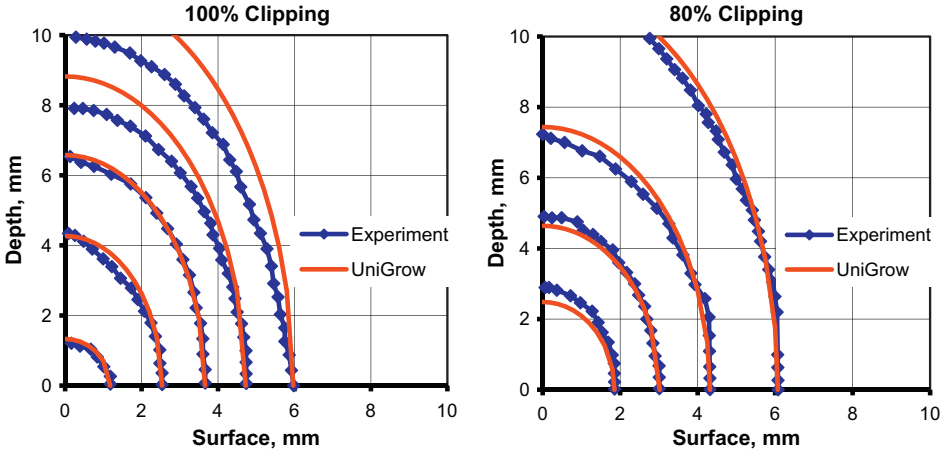

Fig. 14. Experimental and predicted crack shape evolution.

take into account the fact that the correlation between the stress intensity factor and the crack tip stress/strain field is often altered by residual stresses resulting from reversed plastic deformations.

The UniGrow fatigue crack growth model has been subsequently modified and extended by Mikheevskiy and Glinka [6] in order to make it applicable to arbitrary variable amplitude loading spectra. It was found that the instantaneous fatigue crack growth rate depended not only on the residual stresses produced by the latest loading cycle but also on all stress fields generated by preceding cycles of the loading history. In order to combine residual stress fields generated by all preceding loading cycles into one resultant stress field controlling the current fatigue crack growth rate several so-called "memory rules" have been established based on the experimental observations of fatigue crack growth under variable amplitude loading. Detailed description and experimental verifications of the UniGrow fatigue crack growth model in the case of variable amplitude loading spectra can be found in references [5,6,22].

The two parameter driving force (Eq. (13)) is valid for any stress ratio and therefore $da/dN - \Delta K$ fatigue crack growth curves obtained at various R ratios can be approximated by one 'master curve' (Fig. 11) by presenting the fatigue crack growth rate as a function of the total two parameter driving force $\Delta\kappa_{tot}$. The 'master curve' was subsequently divided into two segments and approximated by two linear pieces in the log–log scale by using the linear regression method.

7. Analysis results and discussion

The fatigue crack growth analysis was carried out for the lug subjected to variable loading spectrum described in reference [7] and shown in Fig. 12. The loading spectrum was predominantly tensile with occasional high overloads and underloads.

The data concerning theoretical analysis and the experimental fatigue crack growth through the lug ligament are shown in Fig. 13. The first set of data was obtained from the lug tested under the original loading spectrum. The second loading spectrum, denoted as being 80% clipped, was obtained, according to the nomenclature of reference [7], from the original loading spectrum with all high peaks reduced (truncated) to the 80% of the highest peak in the original (100% clipped) spectrum while all lower stress peaks being unchanged.

The truncation of the loading spectrum from the top reduces residual stresses produced by overloads but also eliminates cycles with high stress intensity ranges and high maxima which may significantly contribute to the fatigue crack propagation. Thus, it was of great interest to find out which effect was dominating. The retardation effect of multiple overloads can be quantified by comparing the fatigue lives corresponding to the truncated loading spectrum with that one obtained under the original loading spectrum. In this particular case the truncation resulted in shorter fatigue life and it was correctly predicted by the UniGrow model. Good agreement between computed and experimentally measured fatigue crack growth (c–N data) indicate that the model correctly simulated the effect of overloads, under-loads and their sequence.

Kim et al. [7] has additionally investigated the corner crack growth by applying marker cycle load with frequency of 100 times per one flight spectrum. He has shown that the distances between beach marks were wider for the 80% clipped spectrum than for the original loading spectrum. This led to shorter fatigue life in the case of the clipped loading spectrum. The experimental beach marks obtained by Kim et al. [7] and the crack shape estimated by the UniGrow fatigue model are shown in Fig. 14. In both cases the calculated crack shape was very similar to that one observed experimentally.

8. Conclusions

The analysis presented in the paper indicates that a variety of effects influencing the fatigue crack growth and resulting from the application of cyclic variable amplitude loading can be modelled by considering the effect of residual stresses in the crack tip region induced by reversed cyclic plastic deformation. The analysis needs to be carried out on cycle-by-cycle basis accounting for each cycle of the applied load/stress history. It has been also shown that the use of appropriate 'memory rules' and the two-parameter driving force enables relatively accurate prediction of fatigue lives of cracked bodies subjected to complex variable amplitude service loading spectra.

The importance of the load shedding in the lug has been quantified by accounting for the decrease of the resultant load in the cracked cross-section. It has been found that the exclusion of this effect in the fatigue crack growth analysis can cause high underestimation of the fatigue crack growth life.

It has been also shown that the weight function technique can be used to obtain stress intensity factor solutions for corner, edge, and transient cracks.

References

[1] Schijve J, Hoeymakers AHW. Fatigue crack growth in lugs. Fatigue Eng Mat Struct 1979;1:185–201.

[2] Smith CW, Jolles M, Peters WH. Stress intensities for cracks emanating from pin-loaded holes flow growth fract. ASTM STP 1977;631:190–201.
[3] Moon JE, Improvements in the fatigue performance of pin loaded lugs. Royal aircraft establishment tech. rept. 80148, 1980.
[4] Rice JR. Some remarks on crack-tip stress field. Int J Solid Struct 1970;46:237–47.
[5] Noroozi AH, Glinka G, Lambert S. A study of the stress ratio effects on fatigue crack growth using the unified two-parameters fatigue crack growth driving force. Int J Fatigue 2007;29:1616–34.
[6] Mikheevskiy S, Glinka G. Elastic–plastic fatigue crack growth analysis under variable amplitude loading spectra. Int J Fatigue 2009;31:1829–36.
[7] Kim Jong-Ho, Lee Soon-Bok, Hong Seong-Gu. Fatigue crack growth behavior of Al7050-T7451 attachment lugs under flight spectrum variation. Theor Appl Fract Mech 2003;40:135–44.
[8] Sharp PK, Byrnes R, Clark G. Examination of 7050 fatigue crack growth data and its effect on life prediction. Airframes and engines division. Aeronautical and maritime research laboratory. Defence Science and Technology Organisation. DSTO-TR-0729.
[9] John R, V Jata K, Sadananda K. Residual stress effects on near threshold fatigue crack growth in friction stir welded aerospace alloys. Int J Fatigue 2003;25:939–48.
[10] Shen G, Glinka G. Weight functions for surface semi-elliptical crack in a finite thickness plate. Theor Appl Fract Mech 1991;15:247–55.
[11] Aberson JA, Anderson JM. Cracked finite-elements proposed for NASTRAN. In: Third NASTRAN User's Colloquium. NASA TMX-2893; 1973. p. 531–50.
[12] Impellizeri LF, Rich D L. Spectrum fatigue crack growth in lugs, in fatigue crack growth under spectrum loads. ASTM STP 1976;595:320–36.
[13] Schijve J, Hoeymakers AHW. Fatigue crack growth in lugs. Fatigue Eng Mater Struct 1979;1:185–201.
[14] Glinka G, Shen G. Universal features of weight functions for crack in mode I. Eng Fract Mech 1991;40:1135–46.
[15] Neuber H. Theory of stress concentration for shear-strained prismatic bodies with arbitrary nonlinear stress–strain law. ASME J Appl Mech 1961;28:544–51.
[16] Forsyth PJE. Unified description of micro and macroscopic fatigue crack behaviour. Int J Fract 1983;5:3–14.
[17] Landgraf RW, Morrow J, Endo T. Determination of the cyclic stress–strain curve. J Mater 1969;4(1):176.
[18] Technical report on low cycle fatigue properties of ferrous and non-ferrous materials. SAE standard J1099. Warrendale (PA); 1998.
[19] Smith KN, Watson P, Topper TH. A stress–strain function for the fatigue of metals. J Mater 1970;5(4):767–78.
[20] Walker EK. The effect of stress ratio during crack propagation and fatigue for 2024-T3 and 7076-T6. ASTM STP 1970;462:1–14.
[21] Dinda S, Kujawski D. Correlation and prediction of fatigue crack growth for different R-ratios using Kmax and $\Delta K+$ parameters. Eng Fract Mech 2004;71:1779–90.
[22] Lee EU et al. Fatigue of 7075-T651 aluminum alloy under constant and variable amplitude loadings. Int J Fatigue 2009;31:1858–64.